Persistence Length of Cylindrical Brush Molecules Measured by Atomic Force Microscopy

Nikhil Gunari, Manfred Schmidt,* and Andreas Janshoff*

Institut für Physikalische Chemie, Johannes-Gutenberg-Universität, Jakob-Welder-Weg 11, 55128 Mainz, Germany

Received July 22, 2005; Revised Manuscript Received January 30, 2006

ABSTRACT: Mechanical properties of single cylindrical polymer brushes with polyisopropylacrylamide (PNIPAM) side chains deposited on mica were probed by atomic force microscopy. Visualization and stretching of individual molecules in aqueous solution clearly reveal the semiflexible nature of the cylindrical macromolecules. Imaging of the brushes on mica and inferring l_p from a $\langle R^2 \rangle$ vs L plot results in an average persistence length of $l_p = 29 \pm 3$ nm, assuming the chains adopt their equilibrium conformation on the surface. Stretching experiments suggest that an exact determination of the persistence length using force extension curves is impeded by the contribution of the side-chain elasticity. Modeling stretching of the cylindrical brush molecule as the extension of a dual chain (side chain and main chain) explains the frequently observed very low persistence lengths arising from a dominant contribution of the side chain elasticity at small overall contour lengths. It is possible to estimate the "true" persistence length of the cylindrical brush molecule from the intercept of a linear extrapolation of a $(l_p^{app})^{-1/2}$ vs L^{-1} plot. By virtue of this procedure a "true" persistence length of 140 nm for the PNIPAM brush molecules was found, which is by far larger than the value obtained from image analysis. This deviation is attributed to the strong surface polymer interactions leading to nonequilibrium conformations of the brush molecules on the mica surface.

Introduction

Manipulation of single molecules by optical tweezers and atomic force microscopy has provided invaluable insight into the elasticity of various macromolecules ranging from nucleic acids,[1,2] polysaccharides,[3] proteins,[4,5] and synthetic polymers[6] to end-grafted polymers.[7] Extension of single macromolecules attached to an AFM tip allows forces to be measured from 10 pN up to several tens of nanonewtons, sufficient to break covalent bonds,[8] while optical tweezers cover the lower force range from 100 fN to 10 pN, rendering both techniques complementary.

Among the different molecules of interest, semiflexible chains are of pivotal importance due to their prevalence in nature. The mechanical properties of molecules such as actin, DNA, and microtubules have attracted extraordinary attention by both experimentalists and theorists strongly based on their function in a living cell associated with mechanical demands.[9,10]

The mechanical behavior of individual semiflexible chains, which are characterized by a persistence length of the same order of magnitude as the contour length, is captured by the wormlike chain (WLC) model.[11,12] The WLC model describes the statistical mechanics of linearly elastic rods, in which the bending energy is quadratic in curvature and where the elastic energy is microscopically a combination of energetic and entropic contributions.

The relevant physical parameter of the WLC model is the persistence length l_p giving an estimate of the length scale over which the tangent vectors along the contour of the chain backbone correlate. Double-stranded DNA, for instance, exhibits a persistence length of ∼50 nm.[13] While excluded-volume effects can safely be ignored if molecules under tension are considered,[14] it is, however, necessary to account for enthalpic stretching in the high force regime as first suggested by Odijk,[15] assuming a cylindrical rod of homogeneous elasticity.

Linear flexible chains with densely grafted linear or dendritically branched side chains exhibit the shape of cylindrical brushes provided that the main chain is much longer than the side chain.[16−21] The properties of the side chains, e.g. chemical structure, dimensions, stiffness, and mutual interaction, are proven to be determining factors for the conformational behavior of the molecule.[16] This opens an opportunity to control the properties of the molecule of interest by synthesizing cylindrical brushes with predefined side-chain characteristics, i.e., to adjust these characteristics by external stimuli, such as the solvent quality, pH, or temperature, and responsive materials may be synthesized accordingly.[17]

The interest in cylindrical brushes is due to conformational effects caused by competition of the entropic restoring force of the extended backbone and the repulsive, steric interaction forces between the side chains. So far, much theoretical attention has been focused on the study of cylindrical brushes in solution, particularly on the conformational properties in terms of main- and side-chain bond angle correlation functions and on the formation of liquid crystalline phases characterized by l_k/d, the ratio of the Kuhn length ($l_k = 2l_p$) to the cross-sectional dimension d of the cylindrical brush polymers. Many experimental studies on various cylindrical brush polymers in solution exist with partly contradictory results concerning the cylinder length per main chain monomer, l, the Kuhn length l_k, and the cross-sectional dimension d.[22−25]

It is therefore of interest to improve the understanding of the mechanical properties of cylindrical brush molecules as a function of side-chain structure and length as well as solvent quality on a single molecule level. Here we present for the first time force−extension experiments using PNIPAM cylindrical brush molecules investigating the entropic and enthalpic restoring forces.

* To whom correspondence should be addressed: Fax +49 6131 3922970; e-mail janshoff@mail.uni-mainz.de; mschmidt@mail.uni-mainz.de.

10.1021/ma0516081 CCC: $33.50
Published on Web 02/24/2006

Experimental Section

Synthesis of cylindrical poly-*N*-isopropylacrylamide brushes by atom transfer radical polymerization using poly-2-bromoisobutyryloxyethyl methacrylate is described elsewhere.[17] The characterization data relevant for the macroinitiator and the polymer brushes as well as a scheme illustrating the synthesis of the brush are compiled in the Supporting Information. For AFM imaging of the PNIPAM brush molecules in air a dilute aqueous solution was spin-cast on freshly cleaved mica (c = 0.1 mg/mL). The molecular architecture of the adsorbed polymer was studied under ambient conditions (air) with a Multimode AFM (Nanoscope IIIa controller, Veeco, Santa Barbara, CA) operating with amplitude feedback in the intermittent contact mode. Silicon tips from Nanosensors (Neuchatel, Switzerland) with a mean radius of ~5 nm, an average spring constant of 42 N/m, and a resonance frequency of 250−300 kHz were used.

For measurements in solution, a droplet of 50 μL of Milli-Q water was placed on a freshly cleaved mica surface and mounted in a homemade AFM PTFE fluid cell. The polymer was dissolved in Milli-Q water and then injected into the fluid cell to roughly achieve the same concentration as the spin-casting solution used for in air measurements. Intermittent contact mode AFM images were obtained in water employing a MFP 3D microscope from Asylum Research, Santa Barbara, CA. V-shaped silicon nitride cantilevers purchased from Olympus (PSA 400) with spring constants in the range of ~0.5 N/m were used for the measurement.

Force spectroscopy measurements were carried out by placing a droplet of 50 μL of the polymer solution (c = 0.1 mg/mL) on freshly cleaved mica and incubated for 1 h. Subsequently, the surface was rinsed with water to remove excess of unbound polymer molecules. Force−distance curves were recorded at 20 °C using the MFP 3D microscope. V-shaped silicon nitride cantilevers purchased from Olympus (PSA 400) exhibiting a nominal spring constant of ~0.01 N/m were used for the pulling experiments. The exact spring constants were determined by thermal noise analysis prior to each experiment.[26]

Results and Discussion

Figure 1a shows an AFM phase image of cylindrical PNIPAM brush molecules adsorbed on mica using intermittent contact mode in air. The molecules were spin-cast at 20 °C from a dilute aqueous solution on a freshly cleaved mica surface. Both the backbone and the tightly adsorbed side chains can be distinguished. The weight-average contour length determined by AFM was calculated to L_w = 110 nm.[17] Figure 1b shows a height image of the cylindrical PNIPAM brushes deposited by adsorption from solution imaged in aqueous solution also using intermittent contact mode exhibiting an average height of 3 nm. Figure 1c displays a typical surface coverage, which has been used for the pulling experiments. A relatively high coverage was chosen in order to increase the probability of observing stretching events.

Experimentally, there are two complementary ways to evaluate the persistence length l_p of the molecules from the AFM images in the framework of the WLC model. One method makes use of the local curvature employing the fact that the bond angle correlation function gives the average cosine angle Θ between the tangents along the brush molecule separated by a distance s:

$$\langle \cos(\Theta) \rangle = e^{-s/l_p} \tag{1}$$

Equation 1 shows that the persistence length l_p is essentially the decay length through which the memory of the initial orientation of the molecule persists.[27]

The second method relies on the equation of Kratky−Porod, which relates the mean-square end-to-end distance $\langle R^2 \rangle$, the

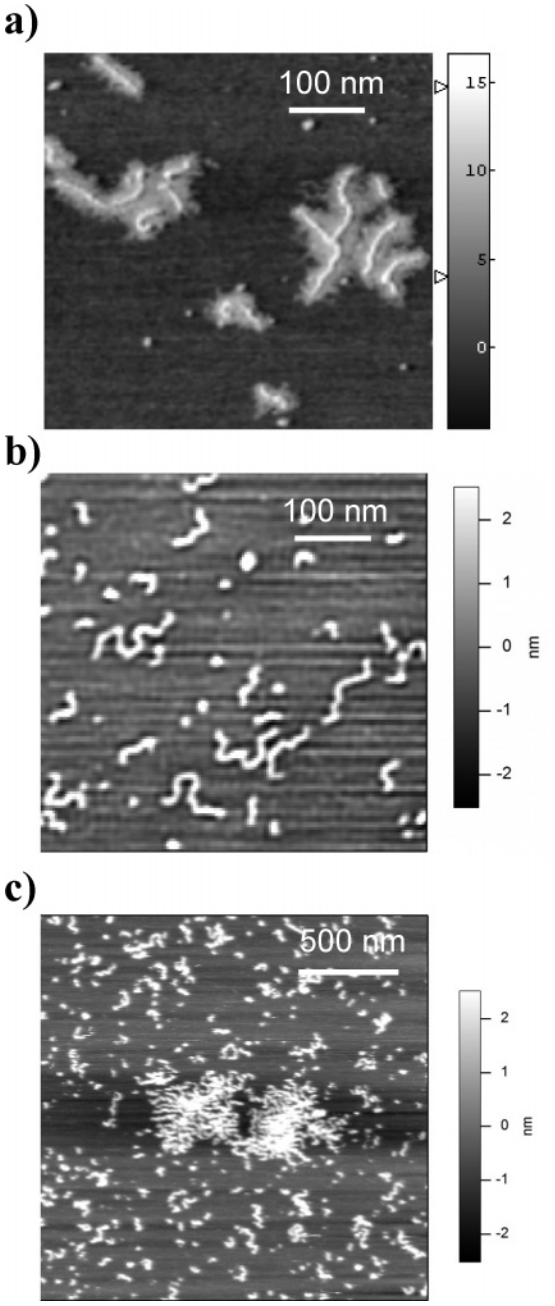

Figure 1. (a) AFM phase image of the cylindrical PNIPAM brushes spin-cast on mica at 20 °C from aqueous solution. (b) Cylindrical PNIPAM brushes imaged by AFM in water also at 20 °C. (c) AFM image of polymer brushes in water showing the typical surface coverage as used for the pulling experiments.

contour length L, and the persistence length l_p in two dimensions (eq 2):[27]

$$\langle R^2 \rangle_{2D} = 4 l_p L \left(1 - \frac{2 l_p}{L} (1 - e^{-L/2l_p}) \right) \tag{2}$$

A different formula results if the molecule on the surface is a projection from 3-D space onto the $x-y$ plane. However, for rigid-rod-like molecules close to the rod limit this equation does not apply.

Figure 2 shows a graph of end-to-end distance $\langle R^2 \rangle$ as a function of contour length as well as the corresponding fit of eq 2. The image size used for the analysis was 1 × 1 μm^2 with 512 × 512 pixels. Bends in the range below 2 nm can thus not be resolved. The persistence length obtained from the fit of eq

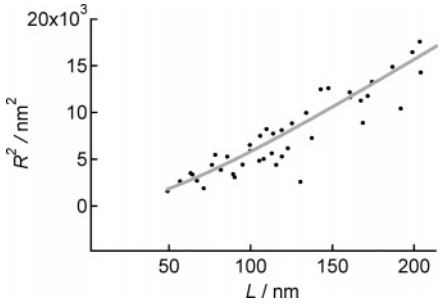

Figure 2. Mean-square end-to-end distance $\langle R^2 \rangle$ as a function of brush contour length L. The continuous gray line is the corresponding fit of eq 2 yielding a persistence length of $l_p = 29 \pm 3$ nm.

2 was $l_p = 29 \pm 3$ nm. In summary, determination of the persistence length using AFM images has a serious drawback related to the interaction of the molecules with the substrate. Bustamante and co-workers recently demonstrated that virtually any conformation of DNA on mica from outstretched to coiled can be obtained by changing the buffer conditions and thus modifying the interaction potential of the surface with the molecule.[28] Molecules might be kinetically trapped or in their equilibrium state. As a consequence, it is appropriate if not necessary to measure force−extension curves of the molecule by employing single molecule force spectroscopy (SMFS), enabling one not only to determine the persistence of the molecule in a more direct manner but also to explore the mechanical properties of the cylindrical PNIPAM brushes in a force regime beyond the purely entropic restoring forces.

Figure 3a−d shows the different classes of events typically observed in stretching adsorbed cylindrical PNIPAM brushes in aqueous solution. A total of $n = 690$ force curves are considered, and only retraction curves are shown in the following graphs. Figure 3a shows a force−extension curve in which no polymer bridge is formed between the tip and the substrate. The absence of stretching events is found in only 15% of all curves. Force−extension curves as displayed in Figure 3b were observed in 38% of the force spectroscopy experiments. The force curve is attributed to the stretching of an individual cylindrical PNIPAM brush molecule displaying a nonlinear extension with force. It is, however, also conceivable that the molecule is picked up in a way that two strands of the same molecule are stretched simultaneously, resulting in an increased persistence length (inset). At high enough extensions, the elastic restoring force of the chain exceeds the physisorption force tethering the molecule either to the tip or to the substrate and the molecule detaches. As shown in Figure 3c, a large number, as high as 30%, of all force−extension curves exhibit desorption events indicative either of the stretching and the subsequent detachment of two physisorbed molecules or might be interpreted as desorption of the molecule from two sites consecutively as illustrated in the inset. 14% of the force curves display multiple detachment events in which more than one or two molecules are involved (Figure 3d). Since the sample is polydisperse and we cannot control the point at which the polymer brush is picked up by the tip, the apparent contour length of the polymer, which is defined as the contour length L_{app} between tip and substrate, varies. The desorption force also varies due to its nonspecific nature and can be as high as 600 pN.

Stiff chains under tension revealing weak undulations are best described by a semiclassical model first introduced by Odijk.[15] Kulic et al. recently presented a different approach in analogy to quantum mechanical tunneling arriving at essentially the same result.[29] For molecules longer than the deflection length $\lambda = \sqrt{k_b T l_p / F} \approx 2-6$ nm and forces larger than $F = k_b T / 4 l_p \approx 0.01$ pN, the following equation holds up to moderate forces:

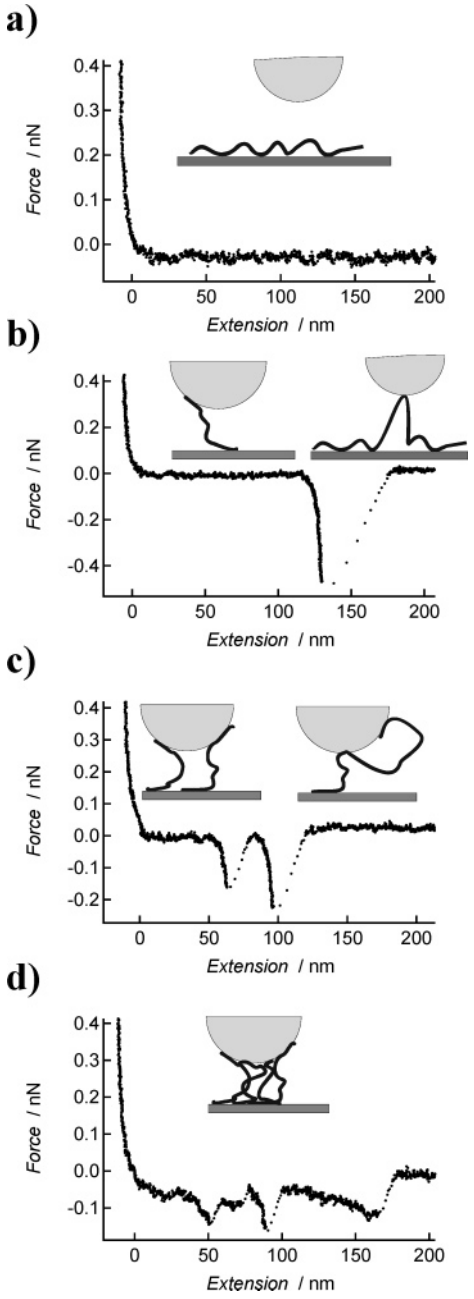

Figure 3. (a) Force−extension curve representing 15% of all curves ($n = 690$) showing no stretching event. (b) Force−extension curve showing a single stretching event attributed to extension of an individual cylindrical PNIPAM brush molecule (38% of the force spectroscopy experiments). (c) Retraction curve exhibiting desorption events indicative of either stretching and detachment of two physisorbed molecules or desorption of the molecule from two sites (30% of all force curves). (d) 14% of all force curves display multiple detachment events in which two or more molecules are involved as shown in the inset.

$$F = \frac{k_b T}{4 l_p} \frac{1}{(1 - x/L)^2} \tag{3}$$

This model describes semiflexible chains under tension as an intermediate between a rigid rod and a flexible coil accounting for both local stiffness and long-range flexibility. The failure of the inextensible model in the high force regime can be attributed to a change from the entropy-dominated restoring forces to the elasticity-dominated regime as the level of stress

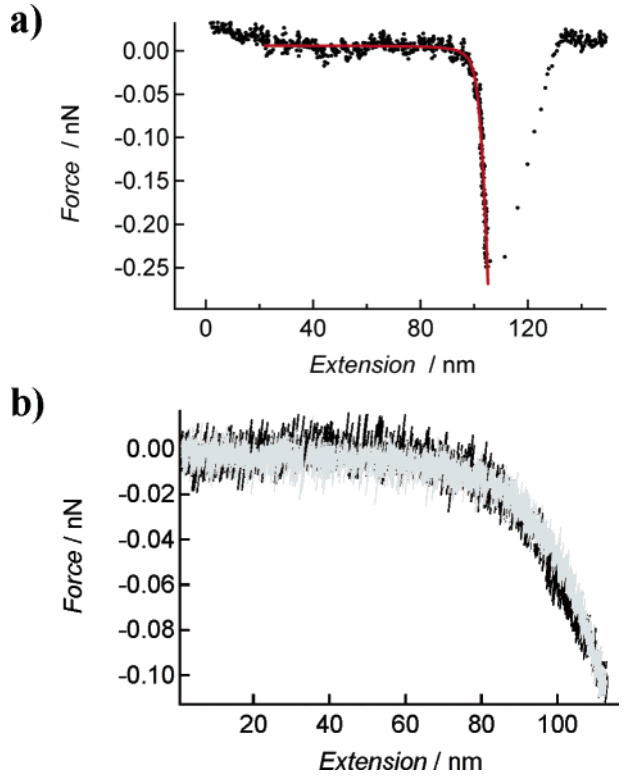

Figure 4. (a) Measured force−extension curve of a cylindrical PNIPAM brush molecule and the corresponding nonlinear curve fit employing the extensible Odijk model (eq 4) providing a persistence length of 23 ± 4 nm and a segment elasticity of 6.5 ± 0.4 nN. (b) Stretching of a single polymer brush without detachment of the molecule. Both relaxation (gray) and extension (black) exhibit the same elasticity, which suggests that adhesion to the surface does not play a dominant role in the force−extension curves.

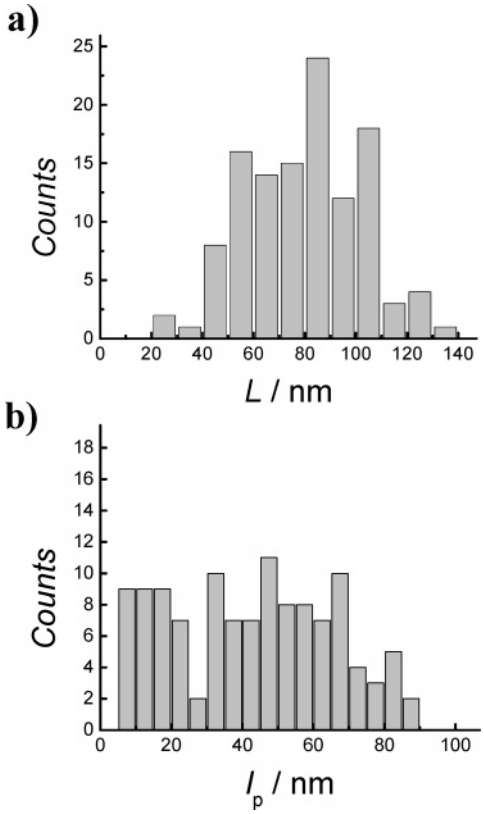

Figure 5. (a) Histogram of extension lengths L with an average apparent contour length of 79 ± 23 nm and (b) histogram of measured persistence lengths exhibiting a mean value of $l_p = 43 \pm 22$ nm.

on the molecule is increased. This infers extension of the molecule beyond its equilibrium contour length. As a consequence, we utilize a modified version of eq 3, the so-called extensible model to fit the persistence length to the data:[15]

$$\frac{x}{L} = 1 - \frac{1}{2}\left(\frac{k_b T}{F l_p}\right)^{1/2} + \frac{F}{\Phi} \qquad (4)$$

Φ denotes the elastic stretch modulus. According to eq 3, x approaches L as $F^{-1/2}$. In this regime the brush molecules can also be enthalpically stretched beyond the contour length L as apparent from eq 4. At $x \geq L$ in the high force regime eq 4 shows approximately linear behavior effectively representing Hooke's law governed by bond angle deformation and bond stretching. In general, there need not be a simple relationship between the stretch modulus and the persistence length. Supposing that the molecule behaves like a cylindrical rod, one might use linear elasticity theory to find $\Phi = 16 k_B T l_p d^{-2}$, leaving Φ in the range of nanonewtons for polymer brushes.[15] Recently, enthalpic stretching of covalent bonds has been quantified as a mixture of bond extension and bending of the bond angles using density functional theory and ab initio approaches. Netz found a stretch modulus of 28 nN for a C−C bond in the trans conformation.[30] Figure 4a shows a nonlinear curve fit employing the extensible Odijk model (eq 4) providing a persistence length of 23 ± 4 nm and a segment elasticity of 6.5 ± 0.4 nN. The extensible model (eq 4) corresponds well to the experimental data in particular in the high force regime, emphasizing that the elasticity of the cylindrical PNIPAM brushes at low forces is dominated by entropic contributions, while in the high force regime the elasticity is governed by enthalpic stretching and deforming of bonds. Fortunately, long-range excluded-volume effects in terms of the ring closure probability do play a role in our case since $L < 3l_p$.

It is instructive to perform continuous stretching experiments with a single chain to prove reproducibility and to gauge the impact of substrate polymer interaction as displayed in Figure 4b. Here, the cylindrical brush molecule has been picked up by the tip extended with a threshold force just below the detachment force and then relaxed without touching the surface. Such a stretching of the suspended molecule is carried out in repeated cycles. We found highly reproducible force−distance curves, i.e., all relaxation and extension curves lie on top of each other, and thus we conclude that interference of the force−extension curve with adhesion of the molecule is highly improbable.

Figure 5 shows two histograms of the apparent persistence length l_p^{app} and the apparent contour length L_{app} obtained by employing the extensible WLC model. A large number (n = 77) of force−extension curves were fitted resulting in an average persistence length of ~40 nm and a number-averaged extension length of 80 nm. The elastic stretch modulus Φ ranges between 2 and 11 nN, in accordance with theoretical models and previous studies.[15,30] The histogram displayed in Figure 5 exhibits a rather broad distribution of apparent persistence lengths l_p^{app}, which might be attributed to two inherent problems associated with pulling at individual brush molecules. First, it is conceivable that side and main chain are extended simultaneously, and second, the attachment of the chain to the tip and surface might reduce the apparent persistence length as first reasoned by Kulic et al.[29]

Stretching of the brush molecule might occur by anchoring of one or more side chains to the tip. As a consequence, main and side chains are extended simultaneously as depicted in

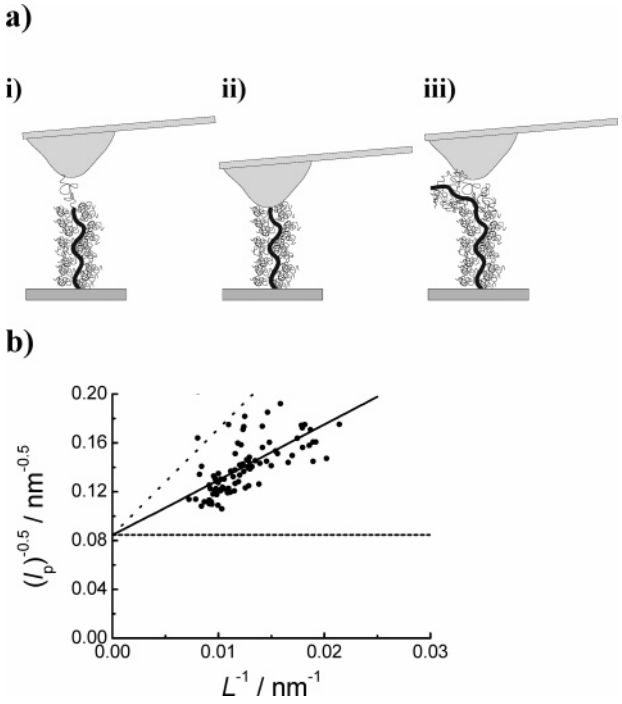

Figure 6. (a) Illustration of different conceivable scenarios when stretching a polymer brush. (i) One side chain is attached to the tip. (ii) Only the main chain is extended between tip and sample. (iii) Several side chains are anchored simultaneously to the tip. (b) Inverse square root of the measured persistence length l_p as a function of inverse extension L. Linear extrapolation (full line) yields a "true" persistence length of $l_{p1} = 140$ nm, assuming an average side chain length of 7 nm and a persistence length l_{p2} of 2 nm following eq 7. The dashed line models a brush pulled only at the main chain, and the dotted line denotes pulling at a side chain exhibiting a length between tip and sample attachment site of 14 nm instead of 7 nm.

Figure 6a, showing different possible scenarios. The restoring force experienced by the cantilever is thus a mixed contribution from stretching the side and main chain, which can be envisioned as two nonlinear springs in series. Hence, the apparent persistence length observed in our experiments might be lowered substantially as compared to those molecules in which merely the main chain is extended by the AFM tip. The decrease of the apparent persistence length is a function of the individual main- and side-chain contour length that is suspended between tip and substrate. The situation gets even more intricate if several side chains are pulled simultaneously each with a different apparent length, which increases the apparent persistence length due to reduction of the force exerted on each side chain.

Stretching of a brush molecule at a single side chain (persistence length: l_{p2}; contour length: L_2) *and* the main chain (persistence length: l_{p1}; contour length: L_1) simultaneously can be described by the extension of two nonlinear chains in series since both chains experience the same force, and thus the overall extension reads

$$x = x_1 + x_2 = L_1 + L_2 - \frac{L_1}{2}\left(\frac{k_bT}{Fl_{p1}}\right)^{1/2} - \frac{L_2}{2}\left(\frac{k_bT}{Fl_{p2}}\right)^{1/2} + \frac{F(L_1 + L_2)}{\Phi} \quad (5)$$

which can be readily cast into an equation yielding an apparent persistence length l_p^{app} and an overall contour length $L_{app} = L_1 + L_2$:

$$\frac{x}{L_{app}} = 1 - \frac{1}{2}\left(\frac{k_bT}{Fl_p^{app}}\right)^{1/2} + \frac{F}{\Phi} \quad (6)$$

The apparent persistence length l_p^{app} as a function of contour length L can be linearized to

$$\frac{1}{\sqrt{l_p^{app}}} = \frac{1}{\sqrt{l_{p1}}} + \left(\frac{1}{\sqrt{l_{p1}}} - \frac{1}{\sqrt{l_{p2}}}\right)L_2 L_{app}^{-1} \quad (7)$$

Hence, a plot of $(l_p^{app})^{-1/2}$ as a function of L_{app}^{-1} provides a means to determine the "true" persistence length of the main chain from a linear approximation and the corresponding y-intercept ($\lim_{L\to\infty}(l_p^{app})^{-1/2} = (l_{p1})^{-1/2}$).

Figure 6b shows a graph displaying the experimentally determined persistence length from fitting eq 5 to each individual force−extension curve as a function of the apparent contour length. Linear extrapolation of the data as justified by eq 7 can be accomplished with a "true" persistence length of 140 nm, an average side-chain persistence length of 2 nm, and a mean side-chain length of 7 nm. The dashed line denotes solely the pulling of a main chain ($l_{p1} = 140$ nm), while the dotted line displays the situation for a longer side chain ($l_{p2} = 2$ nm, $L_2 = 14$ nm) maintaining the parameters for the main chain.

It might also be conceivable that several side chains are extended simultaneously, which diminishes the impact of the side-chain elasticity on the apparent persistence length. Notably, the persistence length of the side chains attached to the tip scales with $nl_p^{sidechain}$, with n the number of side chains with equal length. As mentioned above (Figure 3b (inset)), it might also be possible that the persistence length is larger due to loop formation while picking up the molecule close to the center and thus extending two chains in parallel.

Second, the measured apparent persistence length is also influenced by structural parameters as already pointed out by Marko and Siggia[14] as well as recently shown by Kulic et al.,[29] who found that l_p^{app} decreases according to $l_p^{app} = l_p \cos(\tau)/(1 + cl_p/L)^2$ in which c denotes a structural parameter representing intrinsic bending, loop formation, or the geometry of attachment of the chain to either the substrate or the tip. $\cos(\tau)$ accounts for the direction of force not being collinear with the attachment point of the molecule. As a consequence, deviations from the true persistence length decrease with increasing contour length for such kind of contributions. However, side chains attached to the tip might reduce the impact of attachment geometry on the measured persistence length, rendering this problem of minor importance in our special case.

A "true" persistence length of ~140 nm seems to be rather high as compared to 29 nm obtained from image analysis, assuming that the molecules are in equilibrium on the surface. In fact, a collapse of the PNIPAM brush could not be observed by increase the temperature above the lower critical solution temperature, indicating strong polymer−substrate interactions. Hence, the low persistence length of merely 29 nm might be due to kinetic trapping of the conformation during the adsorption process.

However, a persistence length of 140 nm is higher than expected from common knowledge on cylindrical brushes with different side chain length and with chemically different side chains. Typically, the stiffness of wormlike chains is investigated by static light scattering according to the Benoit−Doty formula, which describes the radius of gyration as a function of the contour length L and of the persistence length l_p. However, for cylindrical brush polymers the contour length is not a priori

known because the cylinder length per main chain repeat unit might be smaller than $l = 0.25$ nm which is usually adopted for vinylic repeat units and because of the contribution of the flexible side chain corona to both ends of the cylindrical brush. Recently combined light and neutron scattering investigations have shown that the cylinder length per repeat unit of the main chain is in fact $l = 0.25$ nm in free solution, in contrast to the much smaller values typically observed by AFM for cylindrical brushes at surfaces.[31] The contribution of the side-chain corona to both ends of cylindrical brushes may be estimated from the formula for the radius of gyration of coil−rod−coil structures derived by Huber.[32] Reevaluation of the LS results given in ref 17 according to the procedure mentioned above and described in some detail elsewhere[33] yields $l_p = 60$ nm, which is about a factor of 2 smaller than that obtained by force spectroscopy. Although this discrepancy appears large at a first glance, it should be noted that for wormlike chains close to the rod limit (i.e., $L/l_p \approx 1-3$) small variations in R_g produce extremely large changes in l_p. For the present data, the change in l_p from 140 to 60 nm produces a variation in R_g by only 17%. Although for the SLS data given in ref 17 this deviation is certainly larger than the experimental error for R_g of about ±5%, a similar sensitivity of the fitted persistence length could be expected for the force−distance curve analysis as well. However, the primary source of uncertainty could originate from the extrapolation procedure shown in Figure 6b. Clearly, much more reliable results could be expected from the investigation of much longer cylindrical brush polymer which, however, are presently not available with PNIPAM side chains.

A possible explanation for the large value of the persistence length might be that the tip occasionally pulls two parts of one chain simultaneously as illustrated in the inset of Figure 3b (right scheme), leading to an inseparable increase in persistence length of the cylindrical brush molecule.

Conclusions

We have directly measured the force vs separation profiles of individual cylindrical PNIPAM brushes as they are extended between an AFM tip and the substrate. The nonlinear force−extension curves are best described by the extensible Odijk model accounting for the deformation of bond angles as well as stretching of the bonds.

Stretching experiments suggest a contour length dependent persistence length, which has been attributed mainly to simultaneously stretching of side chains and main chain. However, the resulting high persistence length of ∼140 nm needs to be verified by other independent methods.

Acknowledgment. We gratefully acknowledge Li Chengming for providing the sample. We also gratefully acknowledge Karl Fischer, Igor Kulic, and Holger Adam for valuable input and fruitful discussions. We thank the DFG for financial support (SFB 625).

Supporting Information Available: Tables of characterization data of PBIEM in THF and of PNIPAM brushes in water; scheme showing the synthesis of macroinitiator and cylindrical PNIPAM brush polymers. This material is available free of charge via the Internet at http://pubs.acs.org.

References and Notes

(1) Bustamante, C.; Marko, J. F.; Siggia, E. D.; Smith, S. B. *Science* **1994**, *265*, 1599−1600.
(2) Rief, M.; Gautel, M.; Schemmel, A.; Gaub, H. E. *Biophys. J.* **1998**, *75*, 3008−3014.
(3) Rief, M.; Oesterhelt, F.; Heymann, B.; Gaub, H. E. *Science* **1997**, *275*, 1295−1297.
(4) Rief, M.; Gautel, M.; Oesterhelt, F.; Fernandez, J. M.; Gaub, H. E. *Science* **1997**, *276*, 1109−1112.
(5) Oesterhelt, F.; Oesterhelt, D.; Pfeiffer, M.; Engel, A.; Gaub, H. E.; D. J.; M. *Science* **2000**, *288*, 143−146.
(6) Ortiz, C.; Hadziioannou, G. *Macromolecules* **1999**, *32*, 780−787.
(7) Zhang, D.; Ortiz, C. *Macromolecules* **2005**, *38*, 2535−2539.
(8) Grandbois, M.; Beyer, M.; Rief, M.; Clausen-Schaumann, H.; Gaub, H. E. *Science* **1999**, *283*, 1727−1730.
(9) Boal, D. *Mechanics of the Cell*, 1st ed.; Cambridge University Press: Cambridge, 2002.
(10) Liu, X.; Pollack, G. H. *Biophys. J.* **2002**, *83*, 2705−2715.
(11) Kratky, O.; Porod, G. **1949**, *68*, 1106−1122.
(12) Kovac, J.; Crabb, C. C. *Macromolecules* **1982**, *15*, 537−541.
(13) Bustamante, C.; Smith, S. B.; Liphardt, J.; Smith, D. *Curr. Opin. Struct. Biol.* **2000**, *10*, 279−285.
(14) Marko, J. F.; Siggia, E. D. *Macromolecules* **1995**, *28*, 8759−8770.
(15) Odijk, T. *Macromolecules* **1995**, *28*, 7016−7018.
(16) Sheiko, S. S.; Möller, M. *Chem. Rev.* **2001**, *101*, 4099−4123.
(17) Li, C.; Gunari, N.; Fischer, K.; Janshoff, A.; Schmidt, M. *Angew. Chem., Int. Ed.* **2004**, *43*, 1101−1104.
(18) Gerle, M.; Schmidt, M.; Fischer, K.; Roos, S.; Müller, A. H. E.; Sheiko, S. S.; Prokhorova, S.; Möller, M. *Macromolecules* **1999**, *32*, 2629−2637.
(19) Sheiko, S. S.; Gerle, M.; Fischer, K.; Schmidt, M.; Möller, M. *Langmuir* **1997**, *13*, 5368−5372.
(20) Zhang, A.; Shu, L.; Bo, Z.; Schlüter, A. D. *Macromol. Chem. Phys.* **2003**, *204*, 328−339.
(21) Schlüter, A. D.; Rabe, J. P. *Angew. Chem., Int. Ed.* **2000**, *39*, 864−883.
(22) Wintermantel, M.; Gerle, M.; Fischer, K.; Schmidt, M.; Wataoka, I.; Urakawa, H.; Kajiwara, K.; Tsukahara, Y. *Macromolecules* **1996**, *29*, 978−983.
(23) Fischer, K.; Schmidt, M. *Macromol. Rapid Commun.* **2001**, *22*, 787−791.
(24) Terao, K.; Nakamura, Y.; Norisuye, T. *Macromolecules* **1999**, *32*, 711−716.
(25) Terao, K.; Hokajo, T.; Nakamura, Y.; Norisuye, T. *Macromolecules* **1999**, *32*, 3690−3694.
(26) Hutter, J. L.; Bechhoefer, J. *Rev. Sci. Instrum.* **1993**, *64*, 1868−1873.
(27) Rivetti, C.; Walker, C.; Bustamante, C. *J. Mol. Biol.* **1998**, *280*, 41−59.
(28) Rivetti, C.; Guthold, M.; Bustamante, C. *J. Mol. Biol.* **1996**, *264*, 919−932.
(29) Kulic, I. M.; Mohrbach, H.; Lobaskin, V.; Thaokar, R.; Schiessel, H. *Phys. Rev. E* **2005**, *72*, 0419051−0419055.
(30) Netz, R. R. *Macromolecules* **2001**, *34*, 7522−7529.
(31) Rathgeber, S.; Pakula, T.; Wilk, A.; Matyaszewski, K.; Beers, K. L. *J. Chem. Phys.* **2005**, *122*, 124904−124917.
(32) Huber, K. *Macromolecules* **1989**, *22*, 2750−2755.
(33) Zhang, B.; Gröhn, F.; Fischer, K.; Pedersen, J. S.; Schmidt, M., manuscript in preparation.

MA0516081